electronics

MDPI

Article

Perylene Based Solution Processed Single Layer WOLED with Adjustable CCT and CRI

Volkan Bozkus, Erkan Aksoy and Canan Varlikli *

Department of Photonics, İzmir Institute of Technology, Urla, 35430 İzmir, Turkey; volkanbozkus@iyte.edu.tr (V.B.); erkanaksoy@iyte.edu.tr (E.A.)
* Correspondence: cananvarlikli@iyte.edu.tr

Abstract: In solution processed single layer white organic light emitting diode (WOLED) applications, the choice of host matrix and optimization of dopant levels represent two crucial parameters to consider. In this work, poly(N-vinylcarbazole) (PVK): 2-(4-Biphenylyl)-5-phenyl-1,3,4-oxadiazole (PBD) and PVK:1,3-bis[(4-tert-butylphenyl)-1,3,4-oxadiazolyl] phenylene (OXD-7) matrices are used as hosts for perylene based devices. PVK:PBD presented better compatibility and lower turn-on voltages compared to PVK:OXD-7. Benefiting from the exciplex emission observed at 630 nm, a color rendering index (CRI) value of 90 is reached with the device containing PVK:PBD as the host and 0.1 wt.% of an orange emitting perylene derivative, i.e., PDI. Introduction of the perylene based green emitter, i.e., PTE, in this emitting layer not only caused a fading in the exciplex emission, but also resulted in disappearance of the electroplex peak at 535 nm, which is detected between PVK:PBD and PTE in bare PTE containing devices. Full visible range coverage is achieved by optimizing the PDI:PTE ratio. WOLED containing PVK:PBD:0.06 wt.% PDI:0.03 wt.% PTE presented high CRI (≥95) and adjustable correlated color temperatures (CCT, 3800 K-5100 K).

Keywords: solution process; WOLED; lighting; perylene derivatives; color rendering index

Citation: Bozkus, V.; Aksoy, E.; Varlikli, C. Perylene Based Solution Processed Single Layer WOLED with Adjustable CCT and CRI. *Electronics* **2021**, *10*, 725. https://doi.org/10.3390/electronics10060725

Academic Editors: Federico Rosei and Geok Ing Ng

Received: 25 February 2021
Accepted: 16 March 2021
Published: 19 March 2021

1. Introduction

Solution processed white organic light emitting diode (WOLED) applications are attracting much attention especially with their easy production process and consequently relatively cost-effective natures [1,2]. It is well known that the quality of the light obtained strongly depends on the balanced electron and hole injection into the emissive layer, exciton formation and its radiative recombination [3]. Utilization of materials with appropriate energy levels, electron and/or hole mobilities and device architecture enhances the electron-hole balance and therefore the exciton formation efficiency. Although triplet sensitizers have the potential of reaching 100% internal quantum efficiency, they suffer from their long exciton diffusion lengths (<100 nm) compared to that of singlet excitons (<20 nm) which retard the radiative recombination step, increase the probability of losses and therefore need more complicated device architectures [4–7]. Recently, singlet emitters, free from those kinds of disadvantages, are getting more and more attention in WOLED applications [8,9].

Besides being a singlet sensitizer, perylene diimides (PDI) have high thermal, optic and chemical stabilities, high fluorescence quantum yields (>90%), and high electron affinities and mobilities [10,11]. All those properties make them very good candidates to be used in WOLED applications. However, due to strong π-π interactions, they tend to form excimer and aggregate in their concentrated solutions (M > [10^{-5}]) and their solution processed films [12–15]. These bottlenecks of PDIs mostly limit their utilization to frequency down-conversion material [16–19]. They are generally introduced into a host matrix [20–24] to obtain electroluminescence (EL) and poly (N-vinylcarbazole) (PVK) represents the most widely used host matrix [25–27]. However, in most of those studies, yellow, red or near infrared EL are presented and only a few of them addressed and yet did not report the main properties of white light altogether [13,28,29]; i.e., (i) the CIE 1931 (Commission

Internationale d'Eclairage) coordinates, (ii) the correlated color temperature (CCT) (cool white > ca. 5000 K and warm white < ca. 5000 K) and (iii) the color rendering index (CRI) > 90 [30–32].

In this study, regular perylene diimide and perylene tetraester derivatives of N,N′-bis(2-ethylhexyl)-3,4,9,10-perylenetetracarboxylic diimide (PDI) and perylene-3,4,9,10-tetracarboxytetrabutylester (PTE) with photoluminescence quantum yields of 93% and 94% in chloroform, respectively [16] are utilized as orange-red and green emitters. They are introduced in PVK dominant host compositions which contain either 2-(4-Biphenylyl)-5-phenyl-1,3,4-oxadiazole (PBD) or 1,3-bis[(4-tert-butylphenyl)-1,3,4-oxadiazolyl]phenylene (OXD-7) as hole blocker and electron transfer materials. It is suggested that red emission intensity is mainly dominated by exciplex formation between the host and PDI, whereas electroplex generation is present for the green region. By optimizing the PDI:PTE ratio in PVK:PBD (60:40 wt.%) host, warm white light with adjustable CCT values (3800 K-5100 K) and CRI value exciding 95 is achieved for a single layer all solution processed perylene based WOLED.

2. Experimental

2.1. Materials

Synthetic, structural, electrochemical, absorption and emission characterization details of the used perylene derivatives of perylene-3,4,9,10-tetracarboxy tetrabutylester (PTE) and N,N′-bis(2-ethylhexyl)perylene-3,4,9,10-dicarboxylic diimide (PDI) are provided at the Supplementary Information (SI) file (Figures S1 and S2) [16,17]. Indium tin oxide (ITO) glass substrates with a sheet resistance of 4–10 Ω/sq, were purchased from Lumtec. Hydrochloric acid (30–32%) [HCl(aq)], poly(3,4-ethylenedioxythiophene):poly(styrene sulfonate) (PEDOT:PSS, Al4083) were from Heraeus Clevios, poly (N-vinylcarbazole) (PVK) (Mw 1.100.000), 2-(4-Biphenylyl)-5-phenyl-1,3,4-oxadiazole (PBD), and 1,3-bis[(4-tert-butylphenyl)-1,3,4-oxadiazolyl]phenylene (OXD-7) were from Sigma Aldrich.

2.2. Methods

UV-Vis absorption and photoluminescence (PL) measurements were performed by using Edinburgh Instruments FS5 spectrophotometer. ITO substrate cleaning was processed by ISOLAB ultrasonic bath and CUTE FC-10046 O_2 plasma system. All solutions were coated via Laurell WS-400B-6NPP LITE spin coater under atmospheric conditions. Film thickness values were determined by KlaTencor MicroXM-100 optical profilometer. Cathode evaporations were performed by the use of a vacuum thermal evaporator attached to a LC Technology Solution Inc. glove box system. The EL spectra and luminance–voltage–current density curves were obtained using a Keithley 2400 source measurement unit and calibrated Hamamatsu C9920-12 measurement system. Frequency varying capacitance values were determined up to 10^6 Hz by using an Agilent 4284A LCR meter.

2.3. Device Preparation

Light emitting layer solutions of x wt.% PDI (x = 0.03, 0.06, 0.1, 0.2, 0.4, 0.6, 0.8, 1.0), y wt.% PTE (y = 0.03, 0.06, 0.1, 0.20) and PDI (x' wt.%): PTE (y' wt.%) (x':y' = 0.1:0.03, 0.1:0.06, 0.1:0.1, 0.06:0.03) were prepared in host matrices of PVK:PBD or PVK:OXD-7 (60:40 wt.%) in chlorobenzene and stirred overnight. Total solution density was kept at 30 mg/mL for each of them. ITO coated glasses were appropriately etched with HCl(aq) and cleaned with detergent, water, deionize water, acetone and isopropyl alcohol, respectively, for 30 min, by using ultrasonic bath. After cleaning, ITO coated glass substrates were treated by O_2 plasma (70 W) for 8 min. PEDOT:PSS was coated by using the spin coater (3000 rpm, 1 min) and annealed at 100 °C for 30 min. Light emitting layers were spin coated on top of PEDOT:PSS at 3000 rpm for 1 min and annealed at 125 °C for 30 min. Finally, LiF (1 nm) and Al (100 nm) cathodes were deposited through a shadow mask and by the use of the vacuum evaporator at 10^{-6} mbar and deposition rates of LiF and Al were 0.2 Å/s and

2.5 Å/s, respectively. The active area of the devices was 7 mm^2 and six parallel devices were fabricated.

3. Results and Discussion

This section may be divided by subheadings. It should provide a concise and precise description of the experimental results and their interpretation, as well as the experimental conclusions that can be drawn.

3.1. Characterization and Determination of Host Matrix

PVK is widely used as p-type host material due to its good film forming properties and compatible energy levels [26,27]. However, because of the low lying HOMO level of PDI (Figure 1), bare PVK cannot be considered an ideal host [20]. Therefore, in order to enhance electronic level alignment and also increase the electron density in the emissive layer, two dopants with different electron mobility values are also introduced in the PVK layer. These materials are PBD and OXD-7 with electron mobility values of 8×10^{-8} cm^2 V^{-1} s^{-1} and $1–4 \times 10^{-5}$ cm^2 V^{-1} s^{-1}, respectively [33]. Energy levels of the materials are depicted in Figure 1 together with the open structures of PDI and PTE.

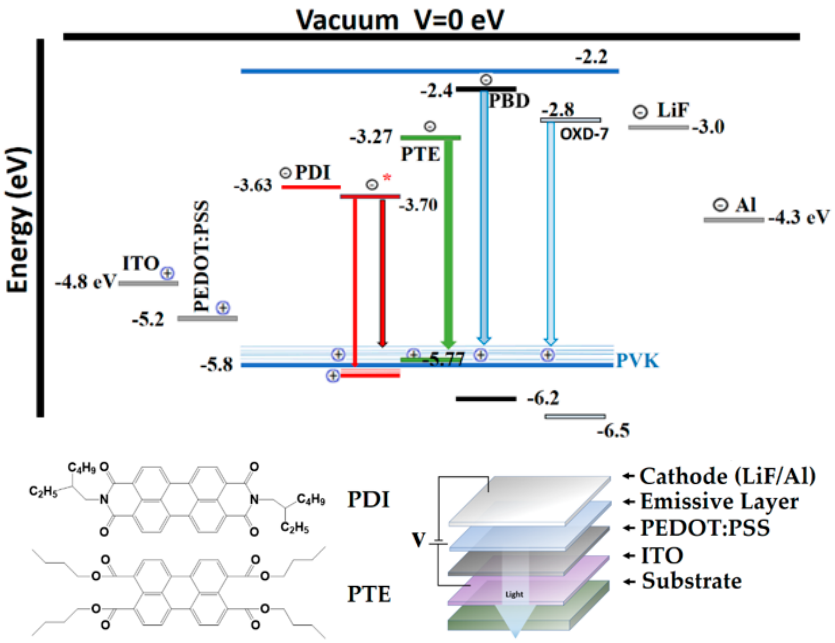

Figure 1. Energy band diagram of the devices, chemical structure of PTE and PDI [energy levels of PVK [25], OXD-7 [34], PBD [35], are taken from literature and PTE and PDI are calculated by using the first reduction potentials and optical band gaps (Figure S2)] and cross sectional view of fabricated device.

PVK:OXD-7 host presented higher turn-on voltages ($V_{turn-on}$) and, lower current density and luminance values (Figure 2a,b) than those of PVK:PBD host in bare PDI containing devices. These results may be attributed to the deeper HOMO and LUMO energy levels of OXD-7, which may act as trap center for the injected holes and may cause unnecessarily excess electron injection in to the emission layer, respectively. Hole mobility values of PVK:PBD and PVK:OXD-7 hosts are calculated to be 2×10^{-6} and 8×10^{-7} cm^2 V^{-1} s^{-1}, whereas the electron mobility values are 8.7×10^{-7} and 1.1×10^{-5} cm^2 V^{-1} s^{-1}, respectively (Figure S3). The dramatic difference obtained between the electron mobility values confirm the above made suggestion on the lower luminance values, but the difference in hole mobility values is incapable of addressing the deeper HOMO level of OXD-7 as the main reason for higher $V_{turn-on}$. The AFM micrographs of PVK:PBD (RMS of 0.31) and PVK:OXD-7 (RMS of 0.44) films presented homogenous and smooth surfaces (Figure S4).

However, dramatic thickness difference between the host media was also detected; the thicknesses of PVK:OXD-7 and PVK:PBD films are 126 ± 4.3 nm and 84 ± 2.0 nm, respectively (Table S1). Therefore, we suggest that in addition to the deeper HOMO energy level, a higher thickness of PVK:OXD-7 layer may have caused charge accumulation on both sides of the active layer and resulted in an increased $V_{turn\text{-}on}$ for the PVK:OXD-7 based OLED [36].

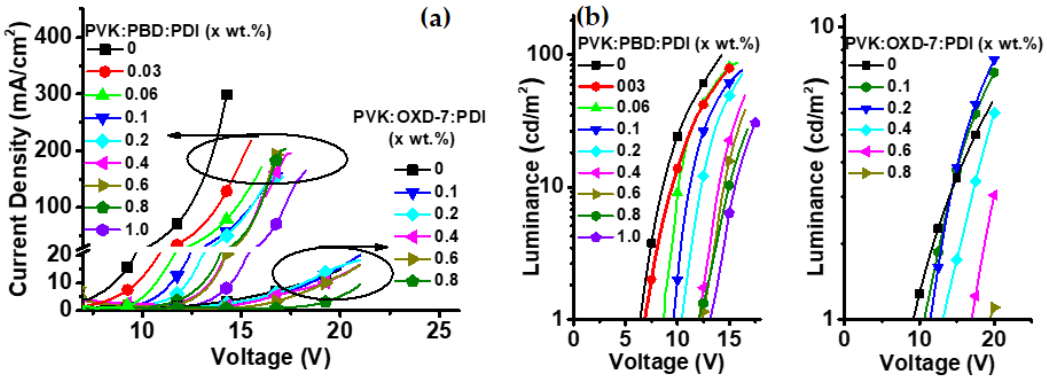

Figure 2. (**a**) Current density—Voltage and (**b**) Luminance -Voltage characteristics of bare PDI devices in host matrices of PVK:PBD and PVK:OXD-7.

The $V_{turn\text{-}on}$ values are increased with the increase in PDI doping wt.% for both of the host media and this increment is more notable with PVK:OXD-7 host (Figure 2b). The explanation given above is also pertinent for the devices those of which PDI doping wt.% is increased. Presence of 0.1 wt.% PDI in PVK:OXD-7 caused approximately 10 nm of thickness increment whereas for PVK:PBD:PDI (0.1 wt.%) this increment is only 5 nm compared to their un-doped films. The thicknesses of PVK:OXD-7: PDI (0.1 wt.%) and PVK:PBD:PDI (0.1 wt.%) films are 135 ± 4.9 nm and 89 ± 3.4 nm, respectively (Table S1). This huge thickness difference is attributed to the different molecular volumes of OXD-7 (378 $Å^3$) and PBD (270 $Å^3$) (molecules are drawn in the chemsketch software and their volumes are calculated by using an online tool [37]). The $V_{turn\text{-}on}$ value increments obtained can also be explained by the high dipole moments and dipole moment differences of the hosts and PDI molecule, which may create energy disorder and consequently reduce the carrier mobility and conductivity of the emitting layer [38].

Due to the comparatively better luminance and lower $V_{turn\text{-}on}$ values obtained, PVK:PBD was chosen as the host matrix. The white light properties of the device structure of ITO/PEDOT:PSS/PVK:PBD:PDI (x wt.%)/LiF/Al are summarized in Table 1. The CIE coordinates of (0.36, 0.29), CCT of 4170 K and CRI of 90 could be reached with 0.1 wt.% PDI doping. Further increment of PDI wt.% caused a reduction in white light properties as a result of decreasing of both the blue and the orange-red emission intensities (Figure S5a).

Table 1. PDI and PTE doping wt.% dependent CRI, CCT and CIE values of ITO/PEDOT:PSS/PVK:PBD:PDI or PTE/LiF/Al devices.

	PVK:PBD:PDI (x wt.%)							**PVK:PBD:PTE (y wt.%)**			
	0.06	0.1	0.2	0.4	0.6	0.8	1.0	0.03	0.06	0.1	0.2
CRI	86	90	82	80	76	74	69	77	74	71	65
CCT	7901	4170	3711	2558	2431	2276	2333	7094	5402	5154	4860
CIE	0.32, 0.26	0.36, 0.29	0.41, 0.34	0.43, 0.35	0.44, 0.35	0.45, 0.35	0.45, 0.35	0.29, 0.37	0.34, 0.42	0.35, 0.45	0.37, 0.49

The EL maximum of PVK:PBD host presented 15 nm of red shift compared to its PL as a result of exciplex emission [39]. The orange-red region of the EL was mainly dominated

by a peak at 610 nm (Figure 3a). Generally, this peak has been observed in PL spectrum of bare PDI films and attributed to aggregation of the PDI core due to π-π stacking [23]. However, 0.1 wt.% of PDI content corresponds approximately 5×10^{-5} M of PDI concentration and aggregation induced PL behavior might not be expected. Therefore, PL measurements are carried on in order to further understand the mechanism and origin of this peak. PL spectra of PVK:PBD:(0.1 wt.%) PDI film presented the same emission wavelength maxima (λ^1_{ems} = 551 nm, λ^2_{ems} = 598 nm and λ^3_{ems} = 650 nm) with the excitation wavelengths of 510 nm and 310 nm which are used for the excitation of the PDI and host, respectively (Figure 3a). Although they preserved characteristic three peak decreasing intensity structure of PDI, λems maxima and PL offset are red shifted approximately 20 nm and 90 nm, respectively, compared to the solution phase ([10^{-6}] in chloroform) and polystyrene (PS): 0.1 wt.% PDI film (Figure S5b). These shifts are evaluated as possible formation of another excited state. Interestingly, in the EL spectrum, λ1ems of PDI was the same while λ^2_{ems} of it also presented approximately 15 nm of red shift and gave a peak at 610 nm. It is deduced that the EL obtained at 610 nm was a result of an excited/ground state energy or charge transfer interaction between the host and PDI. In applied voltage dependent EL measurements [40–42] arising of a new peak at 630 nm is observed and intensities of both the blue and the orange-red regions are affected equally from the voltage increments (Figure 3b). Therefore, it is suggested that the EL at 610 nm was actually the combination of λ^2_{ems} of PDI and exciplex emission with a peak point at 630 nm. This suggestion is supported by the EL intensity increments observed at 630 nm with the increase in PDI doping wt.% in PVK:PBD host system (Figure S5a, inset).

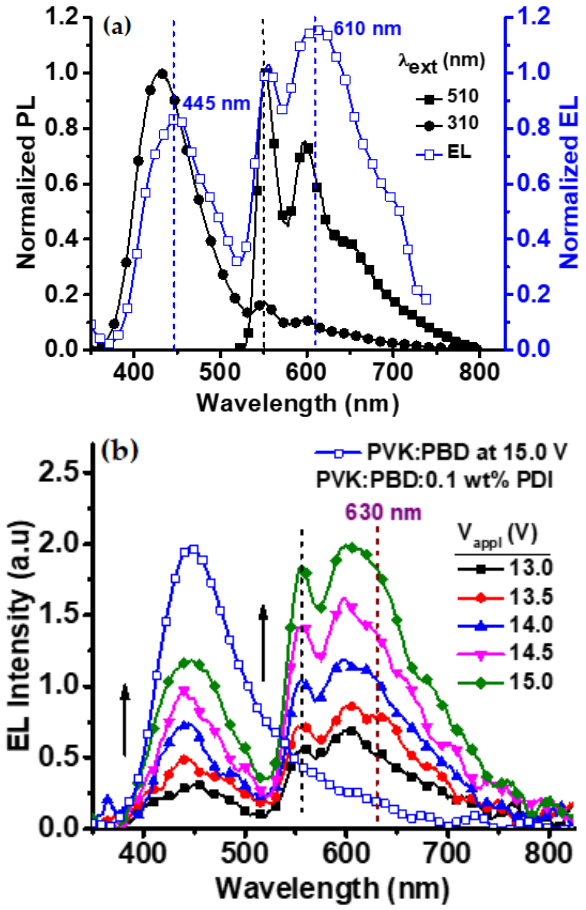

Figure 3. (**a**) Normalized PL and EL spectra of PVK:PBD:PDI (0.1 wt.%) and its corresponding WOLED, respectively and (**b**) EL spectrum of bare PVK:PBD device and applied voltage dependent EL spectra of the device with PVK:PBD:PDI (0.1 wt.%) emitting layer.

3.2. Optimization of White Color Properties

In order to increase the visible light region coverage and consequently, the CRI value of bare orange-red emitting PDI containing devices, green light emitting PTE is thought to be introduced in the emission layer. Absorption and emission spectra of PVK:PBD, PDI and PTE are provided in Figure S2b. Beforehand, the behavior of ITO/PEDOT:PSS/PVK:PBD:PTE (y wt.%)/LiF/Al device is monitored. In a similar manner with the bare PDI devices, the $V_{turn\text{-}on}$ values increased with the increasing doping ratio of PTE (Figure 4a) but the maximum luminance value produced by the bare PTE containing device was slightly higher than that of the bare PDI containing one (Figure 4a vs. Figure 2b). This is attributed to more efficient interaction between the host and PTE due to bigger integral area (overlap) between the absorption of PTE and emission of PVK:PBD compared to that of PDI (Figure S2b). It is well known that in host:guest systems the emission is usually controlled by energy or electron transfer between them [43]. Therefore, in order to determine the measure of transfer, steady state quenching experiments are performed. PDI and PTE are used as quenchers for the emission of PVK:PBD host and quenching rate constants of 9×10^{10} M^{-1} s^{-1} and 3.6×10^{11} M^{-1} s^{-1}, respectively, are extracted from the corresponding Stern-Volmer plots (Figure 4b). These rate constants are higher than the diffusion control limit ($k_q \approx 10^{10}$ M^{-1} s^{-1}) and suggests the probability of charge transfer process between the carbazole based host and perylene derivatives [44].

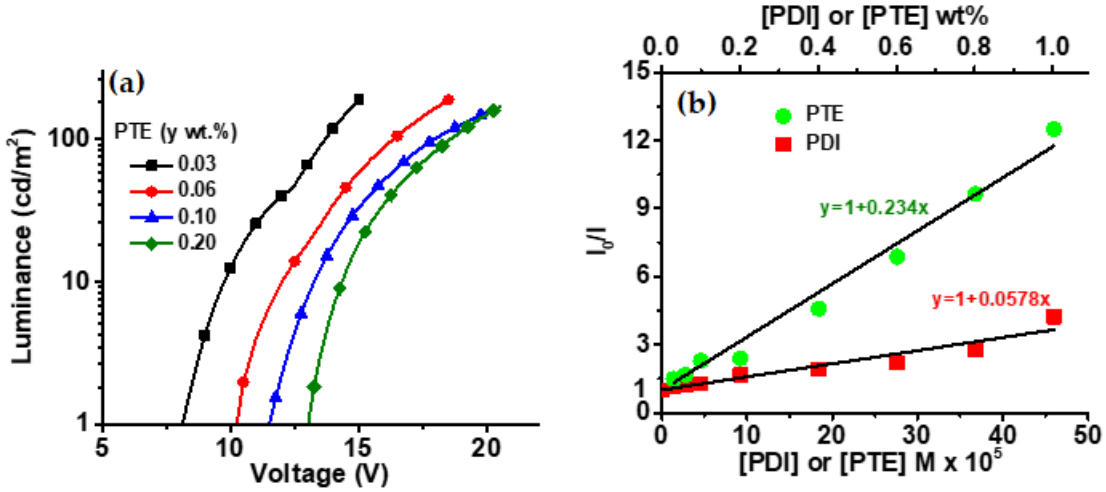

Figure 4. (**a**) Luminance -Voltage characteristics of bare PTE devices in host matrix of PVK:PBD and (**b**) Stern Volmer plot of PVK:PBD PL quenching with the addition of PDI and PTE in film phase [average radiative life time of PVK:PBD is measured as 65 ns (Figure S6)].

Resulting from a better donor-acceptor relationship between the host and PTE, the ratio needed to obtain white light was much lower than that of the PDI based devices. The devices that contain 0.03, 0.06 and 0.1 wt.% PTE presented greenish white light and the CIE values remained above the Planckian locus, while for the bare PDI devices these values are below it (Figure 5). Further increment of PTE wt.% did not cause a significant change in the EL intensities of blue and green regions (Figure 6a). The green region of the EL was dominated by a peak at 535 nm which corresponds to a wavelength of 15 nm red shifted second PL peak of PTE in solution phase (λ^2_{ems} = 520 nm, Figure S2b). The intensity of 535 nm peak is increased with the increase in PTE doping wt.%. Although both the red shift and increasing EL intensity behaviors are similar with the situation in PVK:PBD:PDI devices, it is unlikely that the applied voltage dependent EL spectra presented significant intensity differences between the blue and green regions; the intensity of 535 nm peak increased more than two folds of the 445 nm peak (Figure 6b and Figure S7). Therefore, it is suggested that the EL peak of 535 nm is generated as a result of electroplex formation between the host and PTE [40–42].

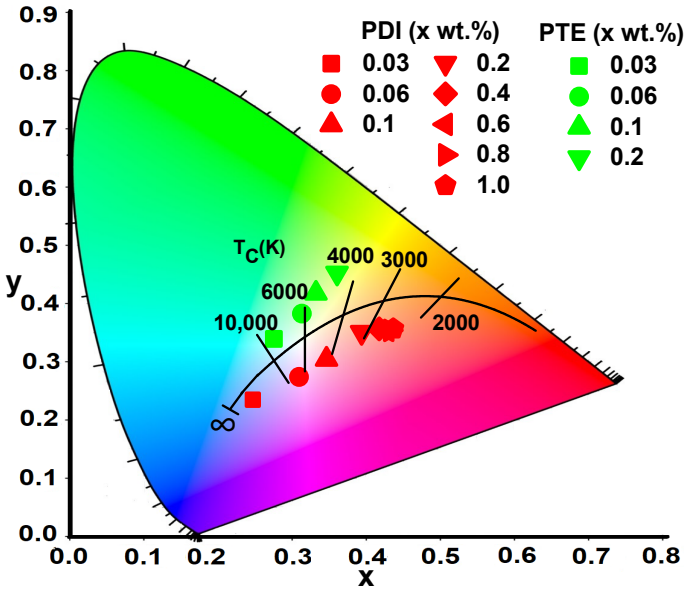

Figure 5. Chromaticity diagram of the devices containing PVK:PBD:PDI and PVK:PBD:PTE emission layers.

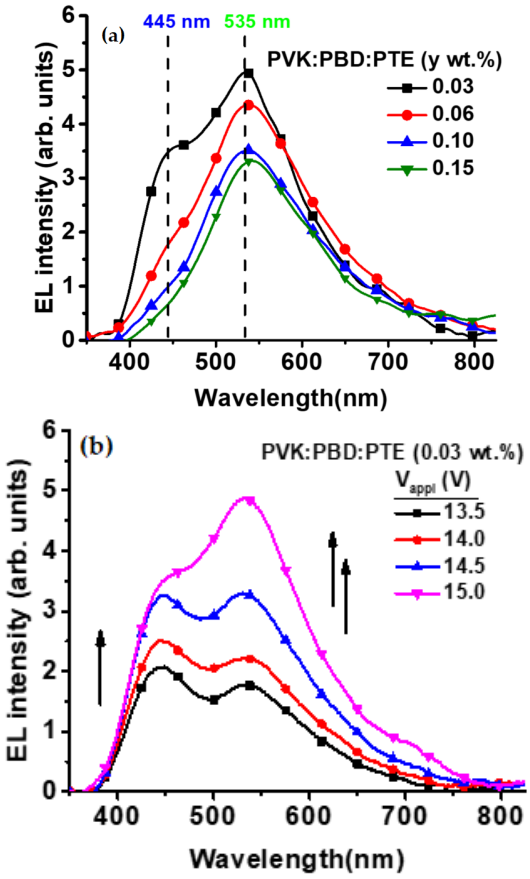

Figure 6. (**a**) EL spectra of PVK:PBD:y wt.%PTE devices and (**b**) applied voltage dependent EL spectra of the device with PVK:PBD:PTE (0.03 wt.%) emitting layer.

The CRI values of PTE containing devices are only around 75 because of the lack of orange-red region and CIE and CCT values of PTE wt.% < 0.1 devices presented the closest values to white light (Table 1). Therefore, these doping ratios of PTE are considered to be introduced in the 0.1wt.%PDI containing device. Device configuration of

ITO/PEDOT:PSS/PVK:PBD:PDI (0.1wt.%): PTE (y' wt.%)/LiF/Al (y' = 0.03, 0.06 and 0.1) is prepared and labeled as Device 1, 2 and 3 in accordance with the increasing y' wt.%. As expected, an increment at the green and a decrement at the blue regions of the EL spectra are detected as the wt.% of PTE is increased (Figure 7a). The fading of 630 nm emission of a bare PDI device and disappearance of the electroplex peak at 535 nm in bare PTE devices are also monitored. The $V_{turn\text{-}on}$ values of Device 1–3 are in the range of bare PDI and bare PTE containing devices. Although the current density at the same applied voltage is in the order of Device 1 > Device 2 ≅ Device 3 (Figure 7b), the EL intensity decrement at 630 nm is continued in Device 2 and Device 3. This situation is evaluated as more evidence of electric field independent formation of 630 nm peak, and the fading is ascribed to the reduction of host concentration ready to form exciplex with PDI as the PTE wt.% is increased. Absence of 535 nm peak is attributed to the wide overlap between the emission of PTE and absorption of PDI (Figure S2).

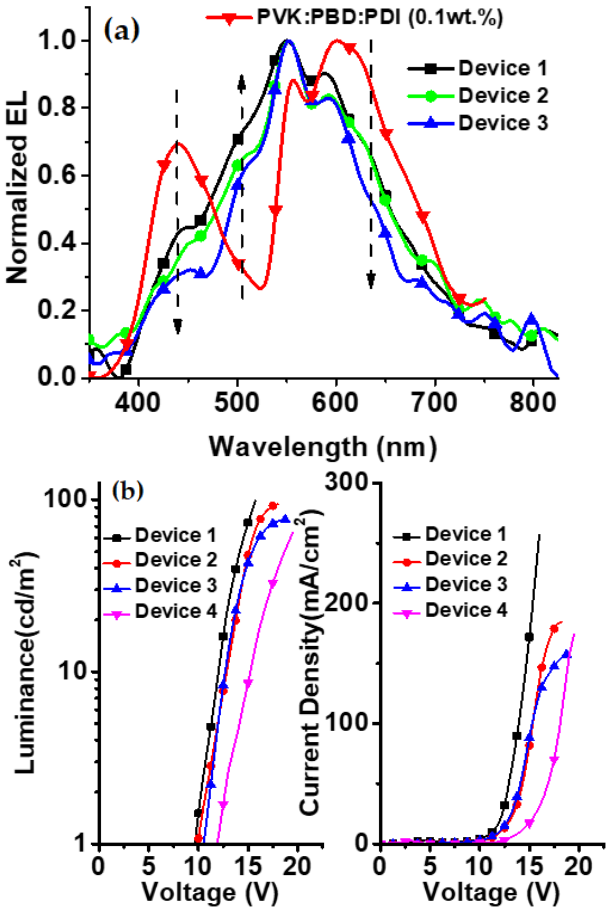

Figure 7. (**a**) Normalized EL curves of Device 1–3 in comparison with normalized EL curve of bare PDI device and (**b**) luminance-voltage and luminance-current density characteristics of Device 1–4 (efficiency curves of Device 1–4 are provided at Figure S8).

The white light properties of Device 1–3 are given in Table 2. Combination of blue, green and orange-red emitter resulted in a CRI value higher than 90. However, white light characteristic is reduced from Device 1 to Device 3. By considering the discussions provided above, in order to regain the green photons absorbed by PDI and increase the host concentration in emitting layer, reducing the PDI wt.% is employed. Device 4, with an emitting layer of PVK:PBD: 0.06 wt.% PDI: 0.03 wt.% PTE, is prepared. Its EL spectrum presented a full visible range coverage (Figure 8) with the combination of dominated peaks at 445, 535, 558 and 620 nm. These peak points are attributed to PVK:PBD, PVK:PBD:PTE electroplex, PDI and addition of PVK:PBD:PDI exciplex and PDI emission

peaks, respectively. Electron (7.3×10^{-7} cm^2 V^{-1} s^{-1}) and hole (8.5×10^{-7} cm^2 V^{-1} s^{-1}) mobility values of this device addressed a balanced charge injection in the emissive layer (Figure S9). White light properties of 96 CRI, 4916 K CCT and (0.34, 0.36) CIE coordinates are achieved (Device #4 in Table 2), which can be manipulated with the applied voltage between 86 and 96, 3800 K and 5100 K, and (0.38, 0.34) and (0.33, 0.40), respectively (Figure S10).

Table 2. CRI, CCT and CIE values Device 1–4 @ maximum brightness.

Device #	CRI	CCT	CIE
1	92	3790	0.37, 0.35
2	90	3773	0.37, 0.36
3	84	4634	0.36, 0.36
4	96	4916	0.34, 0.36

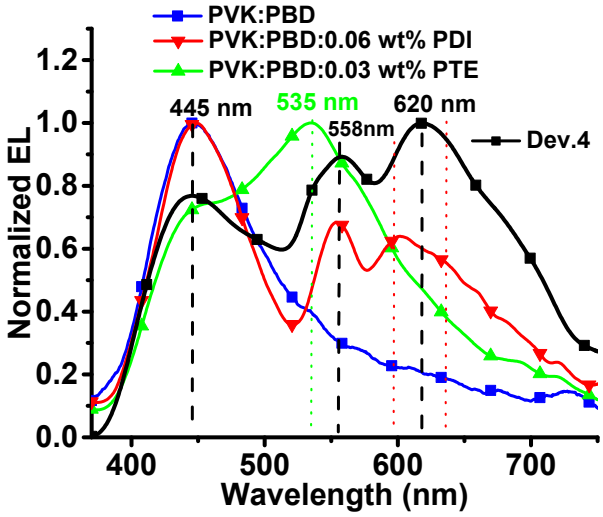

Figure 8. Normalized EL spectrum of Device 4 in comparison with the normalized EL spectra of PVK:PBD, PVK:PBD:(0.03 wt.%) PTE and PVK:PBD:(0.06%) PDI devices.

4. Conclusions

One of the many problems in WOLED generation is the energy transfer between R G B emitters and local color losses. In this study, we produced an optimized host: perylene single layer WOLED with white light properties of 96 CRI, 4916 K CCT and 0.34, 0.36 CIE from selected emitters that prevent aggregation with low doping rates in host [15]. To the best of our knowledge, this device presents the best white light properties of current solution processed single layer perylene based WOLED literature. Comparison of PL and EL spectra of the films and devices, respectively, addressed that the orange-red emission was dominated by the exciplex formation, whereas green emission was mainly generated from the electroplex emission. Energy transfer from the host to the green emitting PTE is more efficient than that of to the orange-red emitting PDI. The lack of the red region resulted in CRI values of only around 75 in bare PTE devices. The highest CRI value obtained with bare PDI devices was 90. Even though the devices do not contain additional layers, optimization of the dopant ratio and detailed investigation of the electronic mechanism during the device operation allowed for reporting the best white light properties of solution processed WOLED literature [28].

Supplementary Materials: The following are available online at https://www.mdpi.com/2079-9292/10/6/725/s1; Synthesis and characterization of perylene derivatives, Figure S1: ^{1}H-NMR spectra of (a) PTE, (b) PDI and (c) FTIR spectrums of PTE and PDI, Figure S2. (a) Cyclic behavior and (b)

absorption spectra of PDI and PTE, electrochemical stability of (c) PTE and (d) PDI, Figure S3. Hole and electron mobility of PVK:PBD and PVK:OXD-7 hosts, Figure S4. (a) AFM images of PVK:PBD and (b) PVK:OXD-7 films, Figure S5. (a) EL vs. wavelength spectra of PVK:PBD:x wt.%PDI devices (inset: EL intensity change at orange-red region for the x values between 0.03 and 0.4) and (b) PL curves of polystyren (PS):PDI (λ_{exc} = 510 nm), PS:PVK:PBD:PDI (λ_{exc1} = 510 and λ_{exc2} = 310 nm), films and PDI solution in $CHCl_3$, Figure S6. Lifetime measurement of PVK:PBD matrix, Figure S7. Applied voltage dependent EL vs. wavelength spectra of PVK:PBD:x wt.%PTE devices (a) x = 0.06 and (b) x = 0.1, Figure S8. (a) External quantum efficiency, (b) current efficiency and (c) power efficiency of Device1–4, Figure S9. Hole and electron mobility of PVK:PBD: 0.06 wt.% PDI: 0.03 wt.% PTE based device; Device 4, Figure S10. (a) Applied voltage dependent CCT and CRI values and (b) CIE coordinate deviation (inset; applied voltage dependent images) of Device 4, Table S1: Thickness measurements of layers.

Author Contributions: V.B.: methodology, validation, formal analysis, investigation (related to device properties) and writing—original draft E.A.: methodology, validation, formal analysis, investigation (related to Synthesis, photophysics and EL mechanisms of perylene derivatives) and writing—original draft C.V.: conceptualization, writing—original draft, review & editing, supervision, project administration. All authors have read and agreed to the published version of the manuscript.

Funding: This research was funded by the Scientific Research Council of Turkey (TUBITAK).

Acknowledgments: We acknowledge the project support fund of the Scientific Research Council of Turkey (TUBITAK) (Project Number: 119F031).

Conflicts of Interest: The authors declare no conflict of interest.

References

1. Guo, F.; Karl, A.; Xue, Q.-F.; Tam, K.C.; Forberich, K.; Brabec, C.J. The fabrication of color-tunable organic light-emitting diode displays via solution processing. *Light Sci. Appl.* **2017**, *6*, e17094. [CrossRef]
2. Tang, C.W.W.; Vanslyke, S.A.A. Organic electroluminescent diodes. *Appl. Phys. Lett.* **1987**, *51*, 913–915. [CrossRef]
3. Zhao, Y.; Chen, J.; Ma, D. Realization of high efficiency orange and white organic light emitting diodes by introducing an ultra-thin undoped orange emitting layer. *Appl. Phys. Lett.* **2011**, *99*, 1–4. [CrossRef]
4. Kim, Y.-H.; Cheah, K.W.; Kim, W.Y. High efficient white organic light-emitting diodes with single emissive layer using phosphorescent red, green, and blue dopants. *Appl. Phys. Lett.* **2013**, *103*, 053307. [CrossRef]
5. Lunt, R.R.; Giebink, N.C.; Belak, A.A.; Benziger, J.B.; Forrest, S.R. Exciton diffusion lengths of organic semiconductor thin films measured by spectrally resolved photoluminescence quenching. *J. Appl. Phys.* **2009**, *105*, 1–7. [CrossRef]
6. Mikhnenko, V.; Blom, P.W.M.; Loi, M.A. Sensitive triplet exciton detection in polyfluorene using Pd-coordinated porphyrin. *Phys. Chem. Chem. Phys.* **2011**, *13*, 14453–14456. [CrossRef]
7. Reineke, S.; Walzer, K.; Leo, K. Triplet-exciton quenching in organic phosphorescent light-emitting diodes with Ir-based emitters. *Phys. Rev. B-Condens. Matter Mater. Phys.* **2007**, *75*, 1–13. [CrossRef]
8. Wu, Z.; Yu, L.; Zhou, X.; Guo, Q.; Luo, J.; Qiao, X.; Yang, D.; Chen, J.; Yang, C.; Ma, D. Management of Singlet and Triplet Excitons: A Universal Approach to High-Efficiency All Fluorescent WOLEDs with Reduced Efficiency Roll-Off Using a Conventional Fluorescent Emitter. *Adv. Opt. Mater.* **2016**, *4*, 1067–1074. [CrossRef]
9. Murawski, C.; Leo, K.; Gather, M.C. Efficiency roll-off in organic light-emitting diodes. *Adv. Mater.* **2013**, *25*, 6801–6827. [CrossRef]
10. Huang, C.; Barlow, S.; Marder, S.R. Perylene-3,4,9,10-tetracarboxylic acid diimides: Synthesis, physical properties, and use in organic electronics. *J. Org. Chem.* **2011**, *76*, 2386–2407. [CrossRef]
11. Li, G.; Zhao, Y.; Li, J.; Cao, J.; Zhu, J.; Sun, X.W.; Zhang, Q. Synthesis, Characterization, Physical Properties, and OLED Application of Single BN-Fused Perylene Diimide. *J. Org. Chem.* **2015**, *80*, 196–203. [CrossRef]
12. Karapire, C.; Kus, M.; Turkmen, G.; Trevithick-Sutton, C.C.C.; Foote, C.S.S.; Icli, S. Photooxidation studies with perylenediimides in solution, PVC and sol–gel thin films under concentrated sun light. *Sol. Energy* **2005**, *78*, 5–17. [CrossRef]
13. Oner, I.; Varlikli, C.; Icli, S. The use of a perylenediimide derivative as a dopant in hole transport layer of an organic light emitting device. *Appl. Surf. Sci.* **2011**, *257*, 6089–6094. [CrossRef]
14. El-daly, S.A.; Fayed, T.A. Diimide in Chloromethane Solvents. *J. Photochem. Photobiol. A* **2000**, *137*, 15–19. [CrossRef]
15. Aksoy, E.; Danos, A.; Varlikli, C.; Monkman, A.P. Dyes and Pigments Navigating CIE Space for Efficient TADF Downconversion WOLEDs. *Dye Pigment.* **2020**, *183*, 108707. [CrossRef]
16. Guner, T.; Aksoy, E.; Demir, M.M.; Varlikli, C. Perylene-embedded electrospun PS fibers for white light generation. *Dye Pigment.* **2019**, *160*, 501–508. [CrossRef]
17. Aksoy, E.; Demir, N.; Varlikli, C. White LED light production by using dibromoperylene derivatives in down conversion of energy. *Can. J. Phys.* **2018**, *96*, 734–739. [CrossRef]

18. Tang, H.; Dong, X.; Chen, M.; Chen, Q.; Ren, M.; Wang, K.; Zhou, Q.; Wang, Z. A novel polymethyl methacrylate derivative grafted with cationic iridium(III) complex units: Synthesis and application in white light-emitting diodes. *Polymers* **2019**, *11*, 499. [CrossRef]
19. Lee, S.H.; Jo, D.S.; Kim, B.S.; Yoon, D.H.; Chae, H.; Chung, H.K.; Cho, S.M. Hybrid color-conversion layers for white emission from fluorescent blue organic light-emitting diodes. *Curr. Appl. Phys.* **2017**, *17*, 1108–1113. [CrossRef]
20. Céspedes-Guirao, F.J.; García-Santamaría, S.; Fernández-Lázaro, F.; Sastre-Santos, A.; Bolink, H.J. Efficient electroluminescence from a perylenediimide fluorophore obtained from a simple solution processed OLED. *J. Phys. D Appl. Phys.* **2009**, *42*, 105106. [CrossRef]
21. Ding, B.; Zhu, W.; Jiang, X.; Zhang, Z. White organic light-emitting diodes based on incomplete energy transfer from perylene to rubrene. *Solid State Commun.* **2008**, *148*, 226–229. [CrossRef]
22. Jeong, C.H.; Lim, J.T.; Kim, M.S.; Lee, J.H.; Bae, J.W.; Yeom, G.Y. Four-wavelength white organic light-emitting diodes using 4,4′-bis-[carbazoyl-(9)]-stilbene as a deep blue emissive layer. *Org. Electron.* **2007**, *8*, 683–689. [CrossRef]
23. Zong, L.; Gong, Y.; Yu, Y.; Xie, Y.; Xie, G.; Peng, Q.; Li, Q.; Li, Z. New perylene diimide derivatives: Stable red emission, adjustable property from ACQ to AIE, and good device performance with an EQE value of 4.93%. *Sci. Bull.* **2018**, *63*, 108–116. [CrossRef]
24. Gupta, R.K.; Ulla, H.; Satyanarayan, M.N.; Sudhakar, A.A. A Perylene-Triazine-Based Star-Shaped Green Light Emitter for Organic Light Emitting Diodes. *Eur. J. Org. Chem.* **2018**, *2018*, 1608–1613. [CrossRef]
25. Gupta, R.K.; Das, D.; Gupta, M.; Pal, S.K.; Iyer, P.K.; Achalkumar, A.S. Electroluminescent room temperature columnar liquid crystals based on bay-annulated perylene tetraesters. *J. Mater. Chem. C* **2017**, *5*, 1767–1781. [CrossRef]
26. Zhang, C.; von Seggern, H.; Pakbaz, K.; Kraabel, B.; Schmidt, H.W.; Heeger, A.J. Blue electroluminescent diodes utilizing blends of poly(p-phenylphenylene vinylene) in poly(9-vinylcarbazole). *Synth. Met.* **1994**, *62*, 35–40. [CrossRef]
27. Zhong, P.L.; Zheng, C.J.; Zhang, M.; Zhao, J.W.; Yang, H.Y.; He, Z.Y.; Lin, H.; Tao, S.L.; Zhang, X.H. Highly efficient ternary polymer-based solution-processable exciplex with over 20% external quantum efficiency in organic light-emitting diode. *Org. Electron.* **2020**, *76*, 1–7. [CrossRef]
28. Gupta, R.K.; Das, D.; Iyer, P.K.; Achalkumar, A.S. First Example of White Organic Electroluminescence Utilizing Perylene Ester Imides. *ChemistrySelect* **2018**, *3*, 5123–5129. [CrossRef]
29. Meng, L.C.; Lou, Z.D.; Yang, S.Y.; Hou, Y.B.; Teng, F.; Liu, X.J.; Li, Y.B. White organic light-emitting diodes based on a combined electromer and monomer emission in doubly-doped polymers. *Chin. Phys. B* **2012**, *21*, 088504. [CrossRef]
30. Pattison, M. Solid-State Lighting 2018 Suggested Research Topics Supplement: Technology and Market Context. 2019. Available online: https://www.energy.gov/sites/prod/files/2019/01/f58/ssl_rd-opportunities_jan2019.pdf (accessed on 30 September 2019).
31. Pattison, M. Solid-State Lighting 2017 Suggested Research Topics Supplement: Technology and Market Context. 2017. Available online: https://www.energy.gov/sites/prod/files/2017/09/f37/ssl_supplement_suggested-topics_sep2017_0.pdf (accessed on 30 September 2018).
32. Kamtekar, K.T.; Monkman, A.P.; Bryce, M.R. Recent advances in white organic light-emitting materials and devices (WOLEDS). *Adv. Mater.* **2010**, *22*, 572–582. [CrossRef]
33. Chang, Y.T.; Chang, J.K.; Lee, Y.T.; Wang, P.S.; Wu, J.L.; Hsu, C.C.; Wu, I.W.; Tseng, W.H.; Pi, T.W.; Chen, C.T.; et al. High-efficiency small-molecule-based organic light emitting devices with solution processes and oxadiazole-based electron transport materials. *ACS Appl. Mater. Interfaces* **2013**, *5*, 10614–10622. [CrossRef]
34. Yang, X.; Wu, F.I.; Haverinen, H.; Li, J.; Cheng, C.H.; Jabbour, G.E. Efficient organic light-emitting devices with platinum-complex emissive layer. *Appl. Phys. Lett.* **2011**, *98*, 033302. [CrossRef]
35. Das, D.; Gopikrishna, P.; Narasimhan, R.; Singh, A.; Dey, A.; Iyer, P.K. White polymer light emitting diodes based on PVK: The effect of the electron injection barrier on transport properties, electroluminescence and controlling the electroplex formation. *Phys. Chem. Chem. Phys.* **2016**, *18*, 33077–33084. [CrossRef] [PubMed]
36. Agrawal, R.; Kumar, P.; Ghosh, S.; Mahapatro, A.K. Thickness dependence of space charge limited current and injection limited current in organic molecular semiconductors. *Appl. Phys. Lett.* **2008**, *93*, 073311. [CrossRef]
37. Jayaram, B.; Singh, T.; Mukherjee, G.; Mathur, A.; Shekhar, S.; Shekhar, V. Sanjeevini: A freely accessible web-server for target directed lead molecule discovery. *BMC Bioinform.* **2012**, *13*, S7. [CrossRef]
38. Friederich, P.; Rodin, V.; von Wrochem, F.; Wenzel, W. Built-In Potentials Induced by Molecular Order in Amorphous Organic Thin Films. *ACS Appl. Mater. Interfaces* **2018**, *10*, 1881–1887. [CrossRef]
39. Jiang, X.; Register, R.A.; Killeen, K.A.; Thompson, M.E.; Pschenitzka, F.; Hebner, T.R.; Sturm, J.C. Effect of carbazole-oxadiazole excited-state complexes on the efficiency of dye-doped light-emitting diodes. *J. Appl. Phys.* **2002**, *91*, 6717–6724. [CrossRef]
40. Wen, L.; Li, F.; Xie, J.; Wu, C.; Zheng, Y.; Chen, D.; Xu, S.; Guo, T.; Qu, B.; Chen, Z.; et al. Electroplex emission at PVK/Bphen interface for application in white organic light-emitting diodes. *J. Lumin.* **2011**, *131*, 2252–2254. [CrossRef]
41. Zhao, D.W.; Xu, Z.; Zhang, F.J.; Song, S.F.; Zhao, S.L.; Wang, Y.; Yuan, G.C.; Zhang, Y.F.; Xu, H.H. The effect of electric field strength on electroplex emission at the interface of NPB/PBD organic light-emitting diodes. *Appl. Surf. Sci.* **2007**, *253*, 4025–4028. [CrossRef]
42. Hao, Y.; Meng, W.; Xu, H.; Wang, H.; Liu, X.; Xu, B. White organic light-emitting diodes based on a novel Zn complex with high CRI combining emission from excitons and interface-formed electroplax. *Org. Electron.* **2011**, *12*, 136–142. [CrossRef]

43. Zeng, H.; Huang, Q.; Liu, J.; Huang, Y.; Zhou, J.; Zhao, S.; Lu, Z. A Red-Emissive Sextuple Hydrogen-Bonding Self-Assembly Molecular Duplex Bearing Perylene Diimide Fluorophores for Warm-White Organic Light-Emitting Diode Application. *Chin. J. Chem.* **2016**, *34*, 387–396. [CrossRef]
44. Kozma, E.; Mróz, W.; Villafiorita-Monteleone, F.; Galeotti, F.; Andicsová-Eckstein, A.; Catellani, M.; Botta, C. Perylene diimide derivatives as red and deep red-emitters for fully solution processable OLEDs. *RSC Adv.* **2016**, *6*, 61175–61179. [CrossRef]